Reprinted from

Tenth International Symposium

Machine Processing of

Remotely Sensed Data

with special emphasis on

Thematic Mapper Data and

Geographic Information Systems

June 12 - 14, 1984

Proceedings

Purdue University
The Laboratory for Applications of Remote Sensing
West Lafayette, Indiana 47907 USA

DIGITAL PROCESSING OF SINGLE-BAND (33.6GHz) MICROWAVE IMAGERY FOR SEA ICE CLASSIFICATION

L.D. FARMER, D.T. EPPLER

Department of the Navy
Naval Ocean Research and Development Activity
NSTL, Mississippi

ABSTRACT

K_a-band brightness temperatures of winter sea ice, acquired using an airborne passive-microwave imager (KRMS), carry sufficient information to segment images into four classes: open water, new ice (frazil), old ice, and first-year ice. Brightness temperatures displayed by new ice and nilas, however, overlap temperatures characteristic of old ice and first-year ice, and limit the utility of classification schemes based solely on K_a-band brightness temperature. Numeric descriptors of texture and shape are required if accurate machine classification of sea ice images is to be achieved.

I. INTRODUCTION

The primary objective of NORDA's K_a-band Radiometric Mapping System (KRMS) program is to develop an operational imaging system that can produce detailed information concerning sea ice conditions over broad regions of the arctic. To this end, methods suitable for automated classification of different ice types from remotely sensed data are being investigated. A plan of experiment has been formulated that will evaluate the feasibility of developing an automated system which, when used in conjunction with airborne K_a-band imagers, will provide these data in real time.

Typical scenes of sea ice include complex assemblages of surface types (Fig. 1). Open water, new ice, nilas, young ice, first-year ice, second-year ice, and multi-year ice occur in close proximity to each other. Previous experiments (Gloersen, et al., 1981; Troy, et al., 1981, 1982; Cavalieri, et al., 1983; Comiso, 1983) suggest that many of these ice types can be distinguished from each other on the basis of their radiometric characteristics at K_a-band frequencies (26.5 to 40.0 GHz) (Fig. 2). Each of these surfaces, then, should be portrayed uniquely in images composed of brightness temperature measurements made within the K_a-band. Conventional, non-numeric methods of image interpretation applied to uncalibrated KRMS images support this conclusion (Ketchum and Lohanick, 1977; Ketchum, et al., 1983).

The simple classification method discussed here is based on K_a-band brightness temperatures alone and represents an initial step toward automated classification of K_a-band images of ice. Our intent is to define the extent to which KRMS brightness temperature data alone, applied without regard to more complex descriptors of texture and shape, can be used to discriminate between winter ice types.

II. INSTRUMENT DESCRIPTION

The KRMS is an airborne passive-microwave imager that operates at a center frequency of 33.6 GHz. The instrument is pod mounted and, in its present configuration, is hung from the bomb bay of an RP-3A aircraft. Three parabolic antennas mounted 120° apart on a single shaft rotate about a horizontal axis within the pod and scan across the flight track. Use of three antennas permits continuous ground coverage to be obtained at flying altitudes above 1000 feet. Although each antenna scans 120° centered at nadir, only 100° of the 120° cross-track scan is used, making cross-track coverage is equal to 2.38 times altitude (725 meters (2380 feet) per 1000 feet of altitude). Antenna

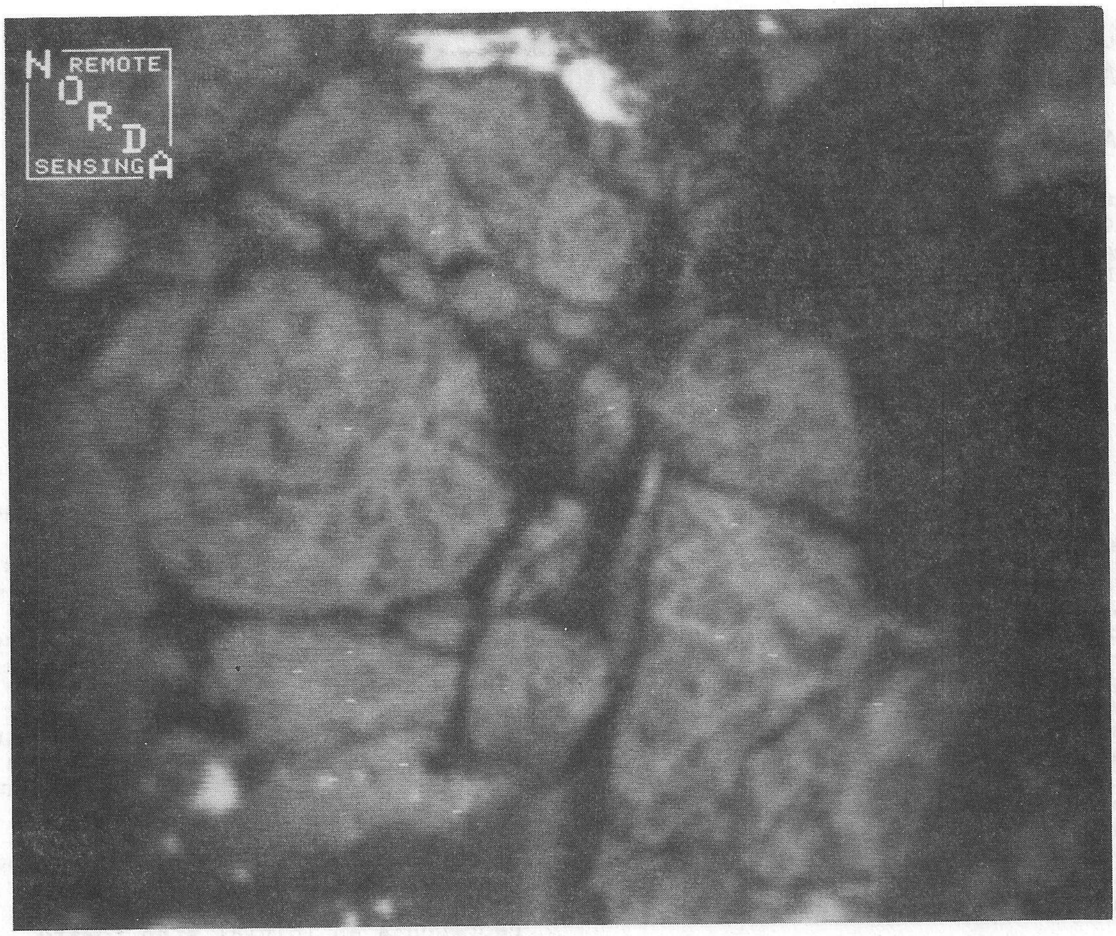

Figure 1. Passive K_a-band image of sea ice. Radiometrically cool surfaces (open water) are depicted by light tones. Radiometrically warm surfaces (first-year ice) are depicted by dark tones. Multi-year ice floes (dappled grey) predominate in the central portion of the scene. A small body of open water (white) is present at top center. First-year ice (black) is present along thu right sidu of the image. New ice and nilas are present at bottom center and along the left margin of the scene. Area imaged is 11,900 feet crosstrack (side to side) by 10,500 downtrack.

beamwidth is 1^{o} so that spatial resolution of the unprocessed signal is 16 feet per thousand feet of altitude. Radiometric sensitivity measured in the laboratory is 0.05 Kelvins/second. Operational sensitivity is 0.5 Kelvins or better. Engineering characteristics of the instrument are given in Table 1.

Microwave radiation emanating from the surface is converted to an RF signal by KRMS electronics and recorded on analog tape in flight. Upon completion of a mission, geometric and radiometric aberrations are corrected and the analog data are converted to digital form (12 bits/pixel, 512 pixels/scan). Signal intensities are calibrated such that they correspond to brightness temperatures (T_B) of imaged surfaces according to procedures described by Eppler, et al. (1984).

III. NUMERICAL IMAGE CLASSIFICATION

Data used for this study were collected on 20 March 1983 from 5000 feet altitude along a track extending 240 miles offshore from Barrow, Alaska. Coincident high resolution aerial photographs (Wild RC-10 mapping camera), surface temperature (thermal) traces (Barnes PRT-5 radiometer), and surface roughness profiles (Spectra-Physics laser profiler) were obtained in conjunction with KRMS data.

Table 1. KRMS Technical Characteristics.

ANTENNAS:		**RF AMPLIFIER:**	
number	3	type	Superheterodyne (DSB)
diameter	24 inches	noise	less than 5.0 db
polarization	vertical	bandwidth	1.3 GHz
beam width	1.0°	gain	greater than 60 db
isolation	40 db (minimum)	loss	1.2 db (maximum)
SCANNNER:		**RADIOMETER:**	
maximum scan rate	25 scans/second (40 ms/scan)	type	pulse stabilized, total power
minimum scan rate	7.5 scans/second (133 ms/scan)	pulse width	4.0 MS
scan angle	$\pm 60^{\circ}$ from nadir	local oscillator frequency	33.6 GHz
midscan incidence angle	0° (nadir)	IF bandwidth	greater than 500 MHz
scan width	3.46 x altitude	video bandwidth	1.7 KHz (maximum)
antenna position accuracy	2.5 minutes of arc	video gain	72 db (nominal)
		minimum detectable signal	0.05 K/second
		sensitivity	50 mv/K (nominal)
		dynamic range	370 K
STABILIZATION:			
method	crosstrack roll gyro		
accuracy	better than 0.25°		

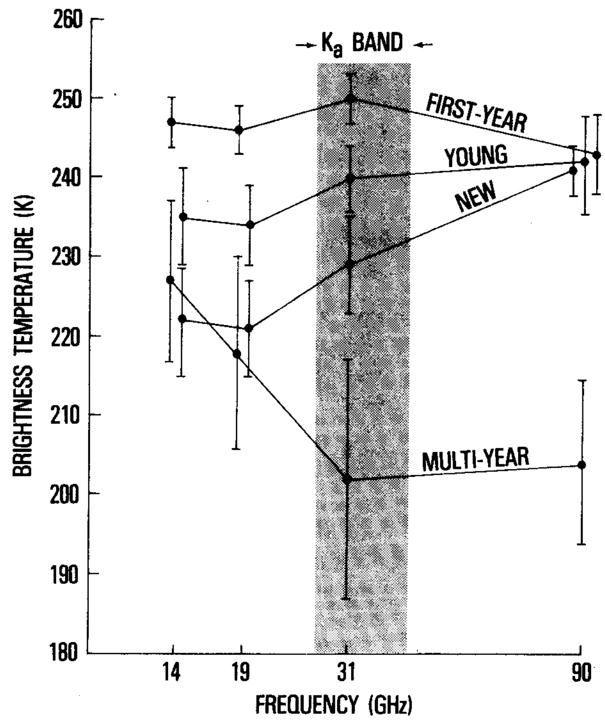

Figure 2. Radiometric brightness temperature as a function of frequency between 14 and 90 GHz for four ice types (from Troy, et al., 1981). Within the range of K_a-band frequencies (shaded), brightness temperatures measured for first-year ice, young ice, new ice, and multi-year ice fall within discrete ranges that do not overlap.

In order to define the radiometric characteristics of different ice types, the frequency distribution of brightness temperatures displayed by training areas encompassing each ice type was determined. Aerial photographs were used to delineate numerous examples of open water, new ice, nilas, young ice, first-year ice, second-year ice, and multi-year ice. Pixel coordinates for each of these training areas were identified on KRMS microwave images. Maximum and minimum brightness temperatures and the mean, variance, and standard deviation of all pixels within each training area were computed. These summary statistics delineate the extent to which winter sea ice can be classified on the basis of K_a-band brightness temperature alone (Fig. 3).

Open water is radiometrically the coldest surface in any of the scenes analyzed. By itself it defines a class characterized by brightness temperatures that fall between 135K (135 Kelvins) and 155K. Temperatures measured for second-year ice and multi-year ice overlap. These two ice types are grouped together to form a second class that consists of old ice. Old ice is characterized by intermediate temperatures that range from 155K to 210K. Temperatures measured for young ice and first-year ice overlap. These two ice types are lumped together to form a third class characterized by radiometrically warm temperatures that fall between 210K and 248K.

Temperature limits for these ice types were used to define breakpoints with which to segment KRMS images into major ice classes. KRMS scenes were classified according to this three-level scheme (Fig. 4). Although open water, first-year ice, and old ice surfaces generally were classified correctly, several shortcomings of the three-level scheme became evident. First, zones of frazil and slush included within areas of open water were classified incorrectly as open water. Therefore, the range of brightness temperatures first assigned to open water (135 to 155 K) was divided into two categories, one from 135K to 145K that corresponds primarily to open water, and another from 145K to 155K that corresponds to frazil and slush.

Second, detail of features within old ice floes and first-year ice and young ice was lost because a single grey tone was used to represent the entire range of brightness temperatures assigned to each category. In terms of digital classification of the images, this is of small consequence. It

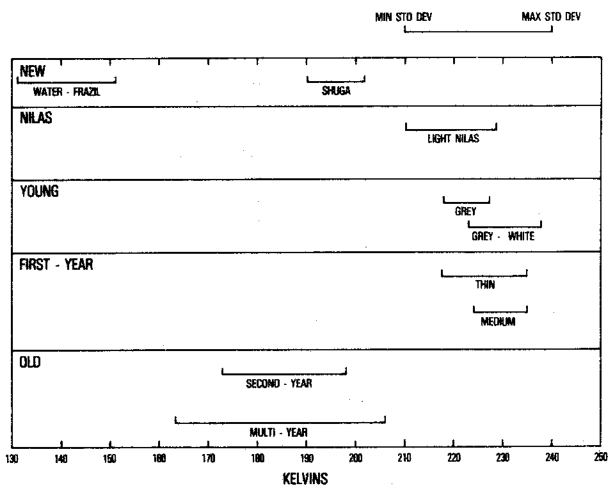

FIGURE 3. Summary statistics for training class data (from Eppler, et al., 1984). The range of values plotted for each ice category is based on statistics calculated for pixel values included in training areas selected for different ice types. The lower end of each bar represents the minimum value calculated for one standard deviation below means of all training areas sampled for each category. The upper end of each bar represents the maximum value calculated for one standard deviation above means for training areas in each category.

detracts, however, from visual analysis of classified images. Therefore, the range of values representative of each class was divided into subclasses along arbitrary temperature boundaries (155K-168K, 168K-183K, 183K-195K, 195K-200K, and 200K-210K for old ice; 210K-219K, 219K-224K, 224K-230K, and 230K-248K for young/first-year ice). Incorporation of these changes results in an eleven-tone image (Fig. 5) in which four types of winter surfaces are segmented: (1) open water, (2) frazil, (3) old ice, and (4) young/first-year ice.

IV. DISCUSSION

Work outlined above defines the extent to which winter ice can be classified if K_a-band brightness temperatures alone are used. Although open water, new ice (frazil), old ice, and young/first-year ice are segmented reliably, second-year ice is indistinguishable from multi-year ice and young ice is indistinguishable from first-year ice. Furthermore, other ice types analysed (new ice and nilas) are characterized by brightness temperature ranges that overlap ranges used to define the four segmented classes (Fig. 3). Temperatures measured for new ice (shuga), for example, coincide with the upper (warm) end of the old ice class; temperatures typical of nilas overlap the lower (cool) end of the young/first-year ice class.

Results of this preliminary study identify areas within the general ice classification scheme in which techniques more sophisticated than brightness temperature analysis must be applied if K_a-band images of ice are to be segmented adequately. Non-numeric methods of image analysis employ visual cues to discriminate between different types of ice. Information concerning overall brightness temperature is supplemented with the shape and texture of ice floes in question. These same functions must be implemented numerically to achieve accuracy comparable to manual methods.

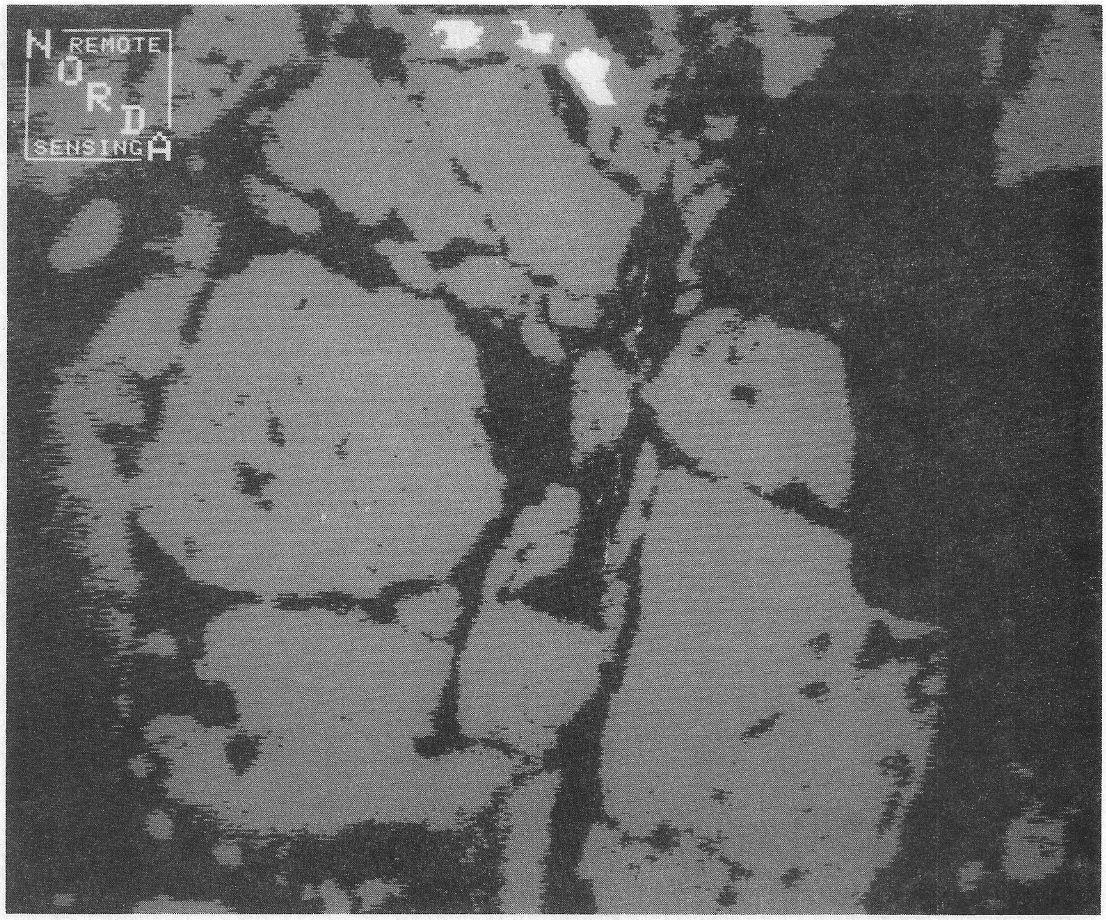

Figure 4. KRMS image segmented into three levels. Open water is white, old ice and most types of new ice are grey, and young ice and first-year ice are black. Image is the same as that shown in Figure 1.

REFERENCES CITED

CAVALIERI, D.J., MARTIN, S., and GLOERSEN, P., 1983, NIMBUS-7 SMMR observations of the Bering Sea ice cover during March, 1979: J. Geophys. Res., v.88, n.C5, p.2743-2754.

COMISO, J., 1983, Sea ice effective microwave emissivities from satellite passive microwave and infrared observations: J. Geophys. Res., v.88, n.C12, p.7686-7704.

EPPLER, D.T., FARMER, L.D., LOHANICK, A.W., and HOOVER, M.C., 1984, Digital processing of passive K_a-band microwave images for sea ice classification: NORDA Tech. Rpt. 51.

GLOERSEN, P., CAVALIERI, D., and CAMPBELL, W.J., 1981, Derivation of sea ice concentration, age and surface temperature from multispectral microwave radiances obtained with the NIMBUS-7 SMMR, in Gower, J.F.R (ed.), Oceanography from Space: Plenum, New York, p.823-829.

KETCHUM, R.D., and LOHANICK, A.W., 1977, Passive microwave signatures of sea ice features: NORDA Tech. Note 9, 16p.

KETCHUM, R.D., FARMER, L.D., and WELSH, J.P., 1983, K-band radiometric mapping of sea ice: NORDA Tech. Note 179, 18p.

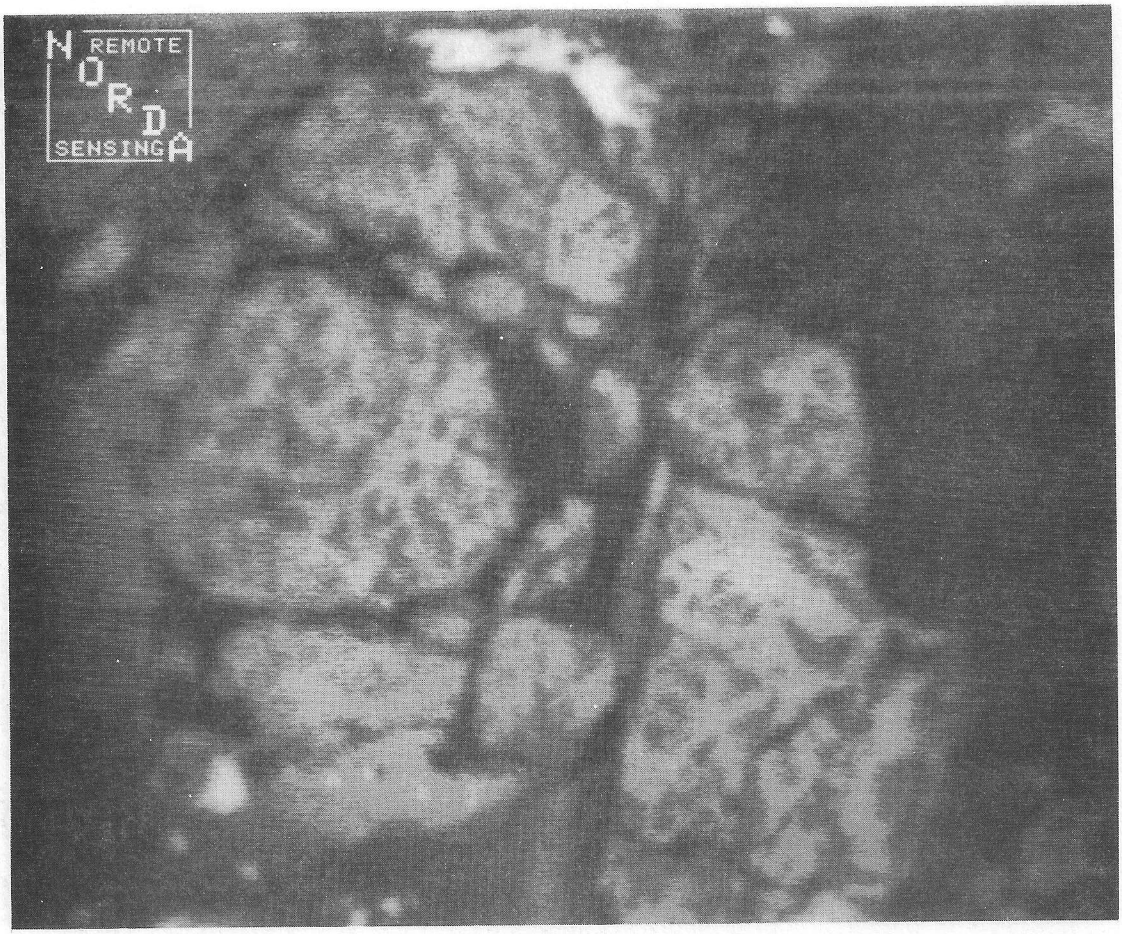

Figure 5. KRMS image segmented into eleven levels.

TROY, B.E., HOLLINGER, J.P., LERNER, R.M., and WISLER, M.M., 1981, Measurement of the microwave properties of sea ice at 90 GHz and lower frequencies: J. Geophys. Res., v.86, n.C5, p.4283-4289.

TROY, B.E., HOLLINGER, J.P., HARTMAN, M.F., RAMSEIER, R.O., and DIGBY, S.A., 1982, Preliminary report of passive microwave and millimeter-wave measurements of Arctic Sea ice, October/November 1981: Naval Res. Lab. Memorandum Rpt. 4861, 134p.

AUTHOR BIOGRAPHICAL DATA

L. Dennis Farmer has worked in remote sensing since 1963, first on active duty with the U.S. Navy (1963 to 1971), then with the U.S. Coast Guard Research and Development Center (1971 to 1978), and finally with NORDA's Polar Oceanography Branch. He served on the crew of the arctic tanker S.S. Manhatten in 1969 and provided navigation guidance from SLAR imagery. He regularly flies remote sensing missions in arctic regions in connection with his present work. He is a member of the American Society of Photogrammetry. Results of his work have been publihed in the Journal of Geophysical Research, the Journal of the American Society of Photogrammetry, and numerous Symposia Proceedings.

Duane T. Eppler worked as a geologist for Texaco, Inc. and as a research associate with West Virginia University before joining NORDA's Polar Oceanography Branch as a geologist. He received a doctrate in geology from the University of South Carolina in 1980. Ongoing research, in addition to digital processing of arctic microwave imagery, include characterization of sea ice from remotely sensed data by analysis of ice floe shape.